The acute phase serum zinc concentration is a reliable biomarker for predicting the functional outcome after spinal cord injury

貴島，賢

The acute phase serum zinc concentration is a reliable biomarker for predicting the functional outcome after spinal cord injury

Ken Kijima [a,b], Kensuke Kubota [c], Masamitsu Hara [b], Kazu Kobayakawa [b], Kazuya Yokota [b], Takeyuki Saito [b], Shingo Yoshizaki [a,b], Takeshi Maeda [c], Daijiro Konno [a], Yoshihiro Matsumoto [b], Yasuharu Nakashima [b], Seiji Okada [a,*]

[a] Department of Pathophysiology, Medical Institute of Bioregulation, Graduate School of Medical Sciences, Kyushu University, Fukuoka, Japan
[b] Department of Orthopaedic Surgery, Graduate School of Medical Sciences, Kyushu University, Fukuoka, Japan
[c] Department of Orthopaedic Surgery, Spinal Injuries Center, Iizuka, Japan

ARTICLE INFO

ABSTRACT

Background: Spinal cord injury (SCI) is a devastating disorder for which the accurate prediction of the functional prognosis is urgently needed. Due to the lack of reliable prediction methods, the acute evaluation of SCI severity and therapeutic intervention efficacy is extremely difficult, presenting major obstacles to the development of acute SCI treatment. We herein report a novel method for accurately predicting the functional prognosis using the acute-phase serum zinc concentration after SCI.

Methods: We produced experimental animal SCI models with different prognoses and examined the relationship among the SCI severity, functional outcome, and acute-phase serum zinc concentration. We also examined whether we could predict the functional prognosis by evaluating the serum zinc concentration within 72 h after SCI in a human prospective study.

Findings: In a mouse model, the acute serum zinc concentrations decreased in proportion to SCI severity and the serum zinc concentrations at 12 h after SCI accurately predicted the functional prognosis. We clarified the mechanism underlying this serum zinc proportional decrease, showing that activated monocytes took up zinc from blood-serum and then infiltrated the lesion area in a severity-dependent manner. A non-linear regression analysis of 38 SCI patients showed that the serum zinc concentrations in the acute-phase accurately predicted the long-term functional outcome ($R^2 = 0.84$) more accurately than any other previously reported acute-phase biomarkers.

Interpretation: The acute-phase serum zinc concentration could be a useful biomarker for predicting the functional prognosis. This simple method will allow for more objective clinical trials and the development of patient-tailored treatment for SCI.

1. Introduction

Traumatic spinal cord injury (SCI) is a devastating event for individuals and causes permanent motor and sensory dysfunction. A number of both basic animal experiments and clinical trials for acute SCI have been conducted to develop effective treatments; however, established treatments are currently limited [1–4]. Since the SCI severity differs considerably from patient to patient and substantial spontaneous functional recovery is often observed during the acute phase of SCI, the prognosis prediction for functional outcome is extremely difficult for acute SCI [5–8]. In fact, even in the mild SCI, severe paralysis was temporarily observed during the very acute phase of SCI, followed by a drastic functional recovery. Therefore, the exact patients matching as well as the precise evaluation of the acute therapeutic intervention efficacy is particularly difficult. In other words, it is unclear how much functional improvement can be attributed to the treatment efficacy or merely to the result of spontaneous functional recovery in clinical trials.

To date, substantial effort has been put into the acute evaluation of SCI severity and predicting the patient recovery potential using serum biochemical markers, imaging analyses, and neurophysiological assessments [9–12]. For instance, Hayakawa et al. reported that the pNF-H in blood was a potential biomarker for evaluating the severity of patients with SCI [13], and Pouw et al. reported S100β as a cerebrospinal fluid (CSF) biomarker [14]. In addition, Matsushita et al. reported that acute-phase magnetic resonance imaging (MRI) findings reflected the neurologic prognosis in patients with SCI [15], and Wilson et al. created

Research in context

Evidence before this study

In traumatic spinal cord injury (SCI), substantial effort has been made for the early evaluation of the SCI severity and prediction of the functional outcome; however, due to the absence of a reliable method for predicting the functional outcome during the acute phase of SCI, accurately evaluating the SCI severity as well as the therapeutic intervention efficacy is extremely difficult. This difficulty constitutes a major obstacle for developing a novel therapeutic strategy for SCI, and therefore, an acute-phase reliable prediction method is urgently needed.
Based on several previous reports, we hypothesize that the inflammatory-related response may be a feasible biomarker for predicting the functional outcome of SCI. Among these responses, we focused on the acute-phase serum zinc concentration since zinc is reported to rapidly redistribute from the blood compartment into cellular compartments during the acute inflammatory phase. In this study, we examined the relationship between the acute-phase serum zinc concentration and the long-term functional outcome after SCI in both an animal experiment and a human prospective cohort study.

Added value of this study

In an animal experiment, we revealed that the acute-phase serum zinc concentration was inversely correlated with the long-term functional outcome after SCI. The mechanism of this association was attributed to the activated infiltrating monocytes, because activated monocytes with SCI took up zinc from the blood serum and then infiltrated the lesion area in a SCI severity-dependent manner, which resulted in a SCI severity-dependent decrease in the serum zinc concentration. Furthermore, a prospective study of 38 SCI patients showed that the acute serum zinc concentration could predict the long-term functional outcome with high accuracy ($R^2 = 0.838$). This prediction accuracy was significantly higher than any other previously reported values.

Implications of all the available evidence

This biomarker will help physicians determine the optimum therapeutic and rehabilitation protocols as well as evaluate the therapeutic intervention efficacy within the very acute phase, contributing to the development of tailored therapeutic approaches for SCI.

a prediction model based on neurological examination variables [16]. However, a limitation of these acute phase studies was that their prediction accuracies were quite low, and there have been no feasible methodologies developed to satisfactorily predict the functional prognosis [17–19]. The inability to reliably predict a patient's potential functional outcome during the acute phase is a major obstacle to the development of therapeutic treatments for acute SCI [20].

After SCI, mechanical trauma rapidly leads to disruption of the blood–spinal cord barrier, neuronal cell death, and axonal damage, followed by a cascade of secondary injuries that expand the inflammatory reaction, which is characterized by immune cell infiltration into the lesion epicenter [21]. We previously demonstrated that the number of infiltrating blood cells in the acute phase of SCI correlated with the SCI severity in a mouse model [19]. In addition, Dalkilic et al. reported that the inflammatory cytokine concentration in the CSF at 24 h after SCI was correlated with the injury severity [12]. These results prompted us to

hypothesize that the inflammatory-related responses may be a feasible indicator for predicting the SCI prognosis. Among them, we focused on the serum zinc concentration because zinc rapidly redistributes from the blood compartment into cellular compartments at the onset of the acute-phase response [22–24]. Indeed, several studies have reported that the blood zinc concentration is inversely correlated with the disease severity under inflammatory conditions, such as sepsis [25–27].

Therefore, in the present study, we examined whether or not there is an association between the SCI severity and blood zinc concentration. In addition, we also investigated the mechanism underlying the association between the acute serum zinc concentration and SCI severity.

2. Materials and methods

2.1. Animals

Female adult C57BL/6 wild-type mice at 8 to 10 weeks of age were used in this study. The mice were kept under constant 12 h light / dark cycle at constant room temperature (23 °C ± 2 °C) while giving food and water ad libitum. Bladder care were performed properly. Animals were excluded from the study if they died, developed infection resistant to antibiotic treatment and/or developed significant autophagia. All animal studies were approved by the Committee of Ethics on Animal Experimentation of our institute and conducted in accordance with the National Institutes of Health guidelines for the care and use of animals. Every effort was made to reduce the number of animals used and to minimize their suffering.

2.2. Spinal cord injury

The mice were anesthetized with an intraperitoneal injection of mixed anesthesia using medetomidine hydrochloride (0·3 mg/kg), midazolam (4 mg/kg), and butorphanol tartrate (5 mg/kg). After laminectomy at the 10th thoracic level, the dorsal surface of the dura mater was exposed, and SCI was induced using an Infinite Horizons Impactor (Precision Systems Instrumentation, Lexington, KY, USA) [28]. With this device, a reliable contusion injury can be created by rapidly applying a force-defined impact with a stainless steel-tipped impounder [29]. Injury with the impactor was performed at force settings of 30, 50, 70, or 90 kdyn. After injury, the overlying muscles were sutured, and the skin was closed with suture wound clips. During recovery from anesthesia, the mice were placed in a temperature-controlled chamber until thermoregulation was re-established. The motor functions were evaluated with the locomotor open-field rating scale of the Basso Mouse Scale (BMS) locomotor rating scales [30]. A team of two experienced examiners evaluated each mouse for 4 min and assigned an operationally-defined score for each hindlimb. The assessment of functional recovery began at 12 h post-injury (hpi). Each mouse was assessed at 12 h, 1 day, 4 days, and 7 days postoperatively and weekly thereafter for 6 weeks. To harvest cell-free serum, 0·6 ml blood was collected via cardiac puncture. After standing upright at room temperature for 30 min and for 6 h at 4 °C, samples were centrifuged at 4000 rpm at 4 °C for 15 min; the supernatant was then quickly removed and stored immediately at −30 °C until further testing. To determine spinal cord zinc concentrations, three spinal cords (2·0 mm in length, centered on the lesion) at 12 hpi were collected and mixed as 1 sample. The zinc concentration of the serum and spinal cord at 12 hpi was determined using the Metallo assay Zn LS Kit (ZN02M, Metallogenics, Chiba, Japan), following the manufacturer's protocol.

2.3. Actual by predicted plot

Actual by predicted plot is a graphical tool for assessing the goodness of model fit. This plot shows the actual Y values on the y-axis and the predicted values on the x-axis. The diagonal line is the Y = X line. If the model fits perfectly, all points are on the diagonal. The red curve

area shows the upper and lower 95% confidence interval. If the red confidence area between the curves contains the blue horizontal line, the model is not significant. If the curves cross the blue line, the model is significant.

2.4. Histopathological examination

At 4 days post-injury, the animals were reanesthetized and transcardially fixed with 4% paraformaldehyde, and thereafter the spinal cord was removed, dehydrated, and embedded in an optimum cutting temperature (OCT) compound. The frozen sections were cut on the sagittal plane at 16 μm. As primary antibodies, rat CD68 (MCA1957GA, 1:200; Serotec, Oxford, UK) and rabbit FluoZin3 (F24195, 10 μM; Invitrogen, Carlsbad, CA, USA) were applied to the sections at 4 °C. The sections were then incubated with Alexa Fluor-conjugated secondary antibodies (1:200; Invitrogen) and Hoechst 33258. All images were captured using a BZ-9000 digital microscope system (Keyence, Osaka, Japan) or epifluorescence microscope equipped with a digital camera (BX51; Olympus, Tokyo, Japan). We measured the number of infiltrating monocyte/macrophages using the US National Institutes of Health ImageJ software program (National Institutes of Health, Bethesda, MD, USA).

2.5. Flow cytometry

Blood and spinal cord samples (6·0 mm in length, centered on the lesion) at 12 hpi were prepared for flow cytometry, as previously described [31]. These samples were stained with anti-CD45 (103,131, Biolegend, San Diego, CA, USA), anti-CD11b (101,211, Biolegend) and anti-Gr-1 (108,415, Biolegend). Cells were then counterstained with FluoZin-3 AM (Invitrogen) or anti-ZIP8 antibody (20459–1-AP, Proteintech, Chicago, IL, USA) and secondary Alexa Fluor 488 antibody (Invitrogen). For ZIP8 counterstaining, leukocytes were fixed with 4% paraformaldehyde and permeabilized with 0.01% Triton X-100 before antibody incubation. The relative levels of intracellular zinc or ZIP8 were compared based on the mean fluorescence intensity (MFI). The samples were analyzed on a FACSAria II flow cytometer (BD Biosciences, San Jose, CA, USA), and the data were analyzed using the FACSDiva software program (BD Biosciences). We calculated the total number of infiltrating monocytes/macrophages within the injured spinal cord.

2.6. Quantitative RT-PCR

Total RNA was isolated from the FACS-sorted monocyte/macrophage obtained from the spinal cord tissue and peripheral blood at 12 hpi using the RNeasy Micro Kit (74,004, Qiagen, Hilden, Germany) and THP-1 cells at 4 h after LPS treatment using the RNeasy Mini Kit (74,104, Qiagen). For complementary DNA (cDNA) synthesis, a reverse transcriptase reaction was performed using a PrimeScript first-strand cDNA Synthesis Kit (6110A, Takara Bio, Otsu, Japan). Quantitative real-time PCR was performed using primers specific to the genes of interest (Supplementary Table 1) and a SYBR Premix Dimmer-Eraser (RR091A, Takara Bio, Shiga, Japan). Data were normalized to the level of glyceraldehyde-3-phosphate dehydrogenase (GAPDH).

2.7. THP-1 cell culture

The human monocytic cell line THP-1 (Japanese Collection of Research Bioresource, Osaka, Japan) was cultured in RPMI medium 1640 with 5% fetal bovine serum, 2 mM L-glutamine, and 1% penicillin-streptomycin. THP-1 cells were treated with LPS at a concentration of 1 μg/ml and incubated for 4 h before immunocytochemical staining, flow cytometry, mRNA extraction, or measuring the zinc concentration, as previously described [32]. For cytoimmunofluorescence staining,

THP-1 cells were incubated with 10 μM FluoZin-3 AM with Pluronic F-127 (P3000MP, Invitrogen) at 37C for 60 min, followed by a confocal microscopy analysis [32].

2.8. Short interfering RNA transfection

A 21-mer short interfering RNA (siRNA) with target sequence directed against human SLC39A8 and scramble siRNA were purchased from Sigma-Aldrich (St. Louis, MO, USA) with the following catalogue numbers: control siRNA: MISSION siRNA Universal Negative Control #1 SIC001; human SLC39A8 siRNA, SASI_Hs02_00355573. The siRNA transfection was performed using the N-TER™ Nanoparticle siRNA Transfection System (Sigma-Aldrich).

2.9. Participants

We recruited 64 SCI patients admitted to the Department of Orthopaedic Surgery at the Spinal Injuries Center (Fukuoka, Japan) between January 2017 and August 2018. Patient data included the age, sex, mechanism of injury, injury level, period from traumatic injury to admission, follow-up period, AIS grade and ASIA motor scores at admission and final follow-up, and serum zinc concentration at admission. The inclusion criteria were as follows: (i) cervical SCI; (ii) 18 years old or older; (iii) admission to our institution within 72 hpi; (iv) undergoing in-patient rehabilitation at our institution; and (v) an adequate assessment with the AIS and ASIA motor score. The exclusion criteria were as follows: (i) death or transfer to another hospital before in-patient rehabilitation; (ii) known or clinical signs of concomitant cerebral damage; (iii) noncooperation with the functional assessment because of dementia; (iv) a history of neurological disorders other than SCI; (v) a history of chronic renal failure; and (vi) hemolytic samples. A total of 38 patients met these criteria, and the AIS as well as ASIA motor scores [33,34] obtained on the final follow-up (mean 6·3 ± 0·8 months) were used as the outcome measurements. All neurological evaluations were performed by senior spinal surgeons at admission and at final follow-up. In addition to these time points, each patient was also evaluated at 4 days, 7 days, 2 weeks, 4 weeks, 6 weeks, and 8 weeks after admission and monthly thereafter. The patient blood samples within 3 days after SCI were collected immediately after being transported to our hospital. To harvest cell-free serum, 4 ml blood was drawn into a sterile tube (Venoject II vacuum blood collection tubes; Terumo, Tokyo, Japan). After standing upright at room temperature for 30 min, samples were centrifuged at 3000 rpm at 4 °C for 5 min; the supernatant was then quickly removed and stored immediately at −30 °C until further testing. Using the Metallo assay Zn LS Kit, the zinc concentration was determined at admission. In our institute, patients with spinal fractures, dislocation, or severe instability undergo surgery. All human study involving the analysis of medical record data was conducted according to the principles expressed in the Declaration of Helsinki and was approved by the Spinal Injuries Center Institutional Review Board. Informed consent was obtained from each subject.

2.10. Statistics

For comparisons of the BMS scores among the four SCI groups, a two-way repeated-measures analysis of variance (ANOVA) with a post-hoc Tukey-Kramer test was performed. Wilcoxon's rank-sum test was used to compare the medians of data from the quantitative PCR analysis, histogram analysis, CD68-positive cells, and culture medium zinc concentrations. For multiple comparisons in culture medium zinc concentration, an ANOVA with Dunnett's post hoc test was applied. Correlational analyses were performed using Pearson's correlation coefficient. In all of the statistical analyses, the level of significance was set

at 0·05. The values for groups are presented as the average ± standard error of the mean. For all box plots, the box includes data points between the 25th to 75th percentiles of all values, with the line inside box representing the median value. The line and whiskers represent data between the 10th and 90th percentiles and the long horizontal line outside box represents mean. All statistical analyses were carried out using the JMP software program (version 13; SAS Institute, SAS Institute, Cary, NC, USA).
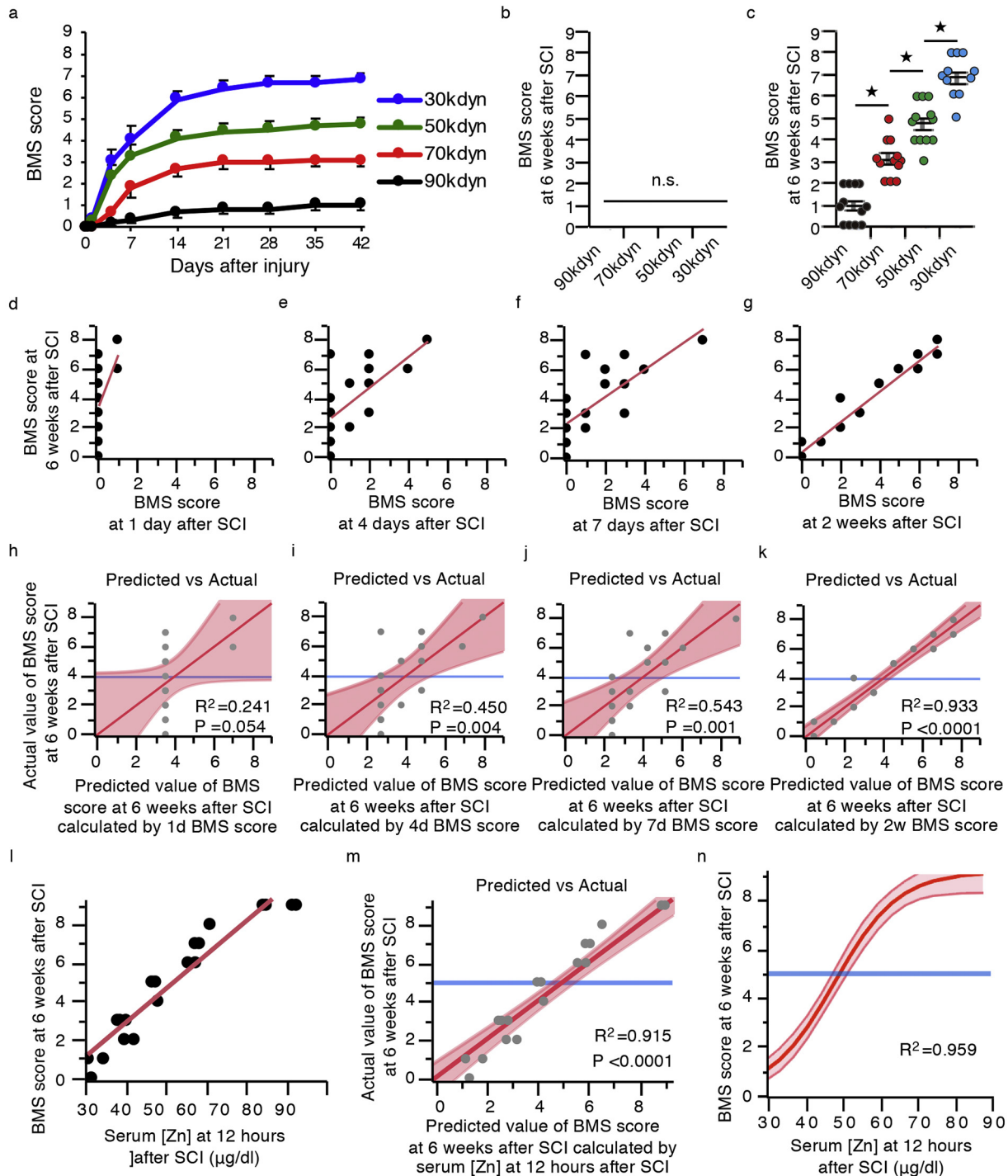

Fig. 1. The serum zinc concentrations at 12 h post-injury (hpi) predict the functional prognosis after mice SCI. (a) The time course of functional recovery according to the BMS score in the 30, 50, 70, and 90 kdyn SCI groups ($n = 12$ mice per group). (b, c) The BMS score from 12 h and 6 weeks after SCI in the 30, 50, 70, and 90 kdyn SCI groups ($n = 10$–12 mice per group). *$P <$ 0.05, ANOVA with the Tukey-Kramer post-hoc test, n.s. = not significant ($P > 0·05$), ANOVA ($n = 10$–12 mice per group). (d-g) Scatter plots illustrating the correlations between the BMS score at 6 weeks post-injury (6 wpi) and at 1 day post-injury (dpi) (d), 4 dpi (e), 7 dpi (f), and 2 wpi (g) ($n = 16$ mice). (h-k) Actual by predicted plot, which plots the observed values of the BMS score at 6 wpi against the predicted values of the BMS score at 6 wpi calculated by the BMS score at 1 dpi (h), 4 dpi (i), 7 dpi (j), and 2 wpi (k) ($n = 16$ mice). (l) Scatter plots illustrating the correlations between the BMS score at 6 wpi and the serum zinc concentration at 12 hpi ($n = 20$ mice). (m) Actual by predicted plot, which plots the observed values of the BMS score at 6 wpi against the predicted values of the BMS score at 6 wpi calculated by the serum zinc concentration at 12 hpi ($n = 20$ mice). (n) The results of the non-linear regression analysis of the functional outcomes using the serum zinc concentration at 12 hpi. Prediction equation: the BMS score at 6 wpi = $9·249 / (1 + EXP\{-0.117[(Zn$ at 12 hpi$) - 48·47]\})$. $R^2 = 0·969$.

3. Result

3.1. Serum zinc concentrations for predicting the functional prognosis after mouse SCI

In order to develop SCI models with different prognoses, we produced four different magnitudes of contusion injury (30, 50, 70, and 90 kdyn) at the 10th thoracic level using a computer-assisted force-defined impactor. In these four groups, both the actual impact force and the calculated displacement were highly reproducible, and there was a strong linear relationship between the actual impact force and the displacement (Pearson: force versus displacement, $R^2 = 0.946$, $p < 0.001$) (Sup Fig. 1). This result was consistent with other reports [28,29].

Although we hardly observed any hindlimb movement until 12 h after injury in all groups, spontaneous recovery was gradually observed over time and plateaued around 2 weeks after injury (Fig. 1a, b). The locomotor function score (BMS score) at 6 weeks after SCI was inversely correlated with the severity of SCI, indicating that we had successfully developed SCI models with different prognoses (Fig. 1c). These result also clearly demonstrated that the injury severity was not synonymous with functional status during the acute phase of SCI.

We next performed a linear regression analysis between the final functional outcome and BMS score at each time point in order to evaluate when we could predict the functional prognoses by assessing the locomotor functional outcomes. After creating the regressed diagonal line by plotting the actual and predicted dots, we calculated the coefficient of determination (R^2). R^2 indicates the proportion that can be explained by the model and ranges from 0 to 1. The results of this linear regression analysis showed the accuracy of the prediction model calculated using the BMS scores at 1 day, 4 days, and 1 week after SCI to be quite low, although the prediction accuracy was significantly high at 2 weeks after SCI (Fig. 1d-k). These findings indicate that predicting the prognosis only by assessing the locomotor function is extremely difficult within the acute phase of SCI. Indeed, the accuracy obtained using several physical examination findings in the acute phase or imaging modalities reported by other studies were also quite low [9,15].

In contrast, the serum zinc concentrations at 12 h after SCI were significantly correlated with the BMS score at 6 weeks after SCI. The results of a linear regression analysis showed that the R^2 calculated by the regression equation was $0 \cdot 915$, which is sufficient for practical use (Fig. 1l, m). In general, the accuracy of a non-linear regression analysis is thought to be higher than that of a linear regression analysis, so we performed a non-linear regression analysis to generate a more accurate model. Consequently, the R^2 calculated by the non-linear regression equation was $0 \cdot 959$ (Fig. 1n). These findings strongly suggest that the acute serum zinc concentration could be a useful and feasible biomarker for predicting the functional prognosis in acute SCI.

3.2. SCI induces zinc influx into infiltrating monocyte, resulting in decreased serum zinc concentration

To clarify the mechanism by which the acute serum zinc concentration is inversely correlated with the SCI functional prognosis, we examined both serum and injured spinal cord zinc concentrations in the SCI models with different prognoses. Interestingly, at 12 h after SCI, the acute serum zinc concentration was negatively correlated with the SCI severity (Fig. 2a), whereas a significantly positive correlation was noted between the SCI severity and zinc concentrations in the injured spinal cord (Fig. 2b). Given that zinc is an essential trace element that cannot be synthesized in the body, we hypothesized that infiltrating cells from the peripheral blood into the injured spinal cord might be involved in the changes in the zinc concentrations.

Since we previously demonstrated that neutrophils and monocytes infiltrated the injured spinal cord from the peripheral blood in the acute phase of SCI [31], we selectively isolated neutrophils and monocytes from both the peripheral blood and injured spinal cord using a cell sorter. In brief, neutrophils were selectively isolated as a CD11b-high/Gr-1high population and monocyte as a CD11bhigh/Gr-1nega-int/CD45high population (Sup Fig. 2). Thereafter, the intracellular zinc concentration levels in both isolated neutrophils and monocytes were compared using the cell-permeable zinc indicator FluoZin-3 based on their MFI. Consequently, although the intracellular zinc levels in infiltrated neutrophils were comparable to those of neutrophils in naïve peripheral blood (Fig. 2c), the levels in infiltrated monocytes were significantly increased compared to those of monocytes in naïve peripheral blood (Fig. 2d). In addition, zinc level of monocytes in the peripheral blood of SCI mice showed bimodal distribution, and the zinc level of each population was comparable level of infiltrated monocytes isolated from injured spinal cord and peripheral blood monocytes in naïve mice, respectively. This result indicated that only monocytes which took up zinc from serum blood infiltrated into the injured spinal cord (Fig. 2e). Furthermore, we also found that the expression of the zinc importer SLC39A8 (ZIP8) in infiltrated monocytes was significantly increased compared to peripheral blood monocytes in naïve mice (Fig. 2f). Consistent with this result by flow cytometry, quantitative RT-PCR showed that the gene expression of ZIP8 was increased in monocytes without significantly altering the expression of the 13 other ZIPs after SCI (Fig. 2g). These results indicate that the ZIP8 expression and zinc influx were enhanced in the infiltrating monocytes after SCI, resulting in a decrease in the zinc concentrations in serum and an increase in the zinc concentrations in injured spinal cord.

3.3. The number of infiltrating monocytes is dependent on SCI severity

Significant correlations between the SCI severity and decreased serum zinc concentrations as well as increased zinc concentrations in injured spinal cord prompted us to hypothesize that the number of infiltrating monocytes is critical for predicting the SCI severity. We therefore examined the relationship between the SCI severity and the number of infiltrating monocytes in injured spinal cord using flow cytometry and found a clear proportional relationship between them (Fig. 3a). In addition, an immunohistological analysis showed that the number of CD68-positive monocytes depended on the SCI severity and that these monocytes were FluoZin3-positive (Fig. 3b-d). Similar results were obtained by counting the number of P2ry12-negative and CD68-positive cells (Sup Fig. 3a, b). These results indicate that the number of infiltrating monocytes that took up zinc from the serum blood increased in proportion to the SCI severity, resulting in a proportional increase in the spinal cord zinc concentration as well as a proportional decrease in the serum zinc concentration.

To further evaluate whether the zinc has the direct effect on the secondary damage such as cell death, we directly injected zinc or saline into the normal spinal cord and examined the gene expression changes. As a result, we found that the expressions of apoptosis-related gene (TNF-α, Fas, Caspase8) did not exhibit any change at 12 h after zinc was administered (Sup Fig. 4a). In contrast, when the activated monocytes which were sorted by FACS from injured spinal cord at 12 h after SCI were transplanted into normal spinal cord, we found that the expressions of apoptosis-related gene were significantly increased in proportion to the number of transplanted monocytes (Sup Fig. 4b). These results suggest that the secondary damage after SCI is associated with the monocyte-mediated inflammation rather than the zinc toxicity.

3.4. Zinc concentration in the culture medium decreases in cell number-dependent manner

SCI mechanical trauma rapidly leads to disruption of the blood–brain barrier, neuronal cell death, edema, axonal damage, and demyelination, followed by a cascade of secondary injuries that expand the inflammatory reaction, which is characterized by immune cell infiltration and the activation of systemic immunity at the epicenter of the injury [21]. To determine whether or not proinflammatory stimuli induce ZIP8
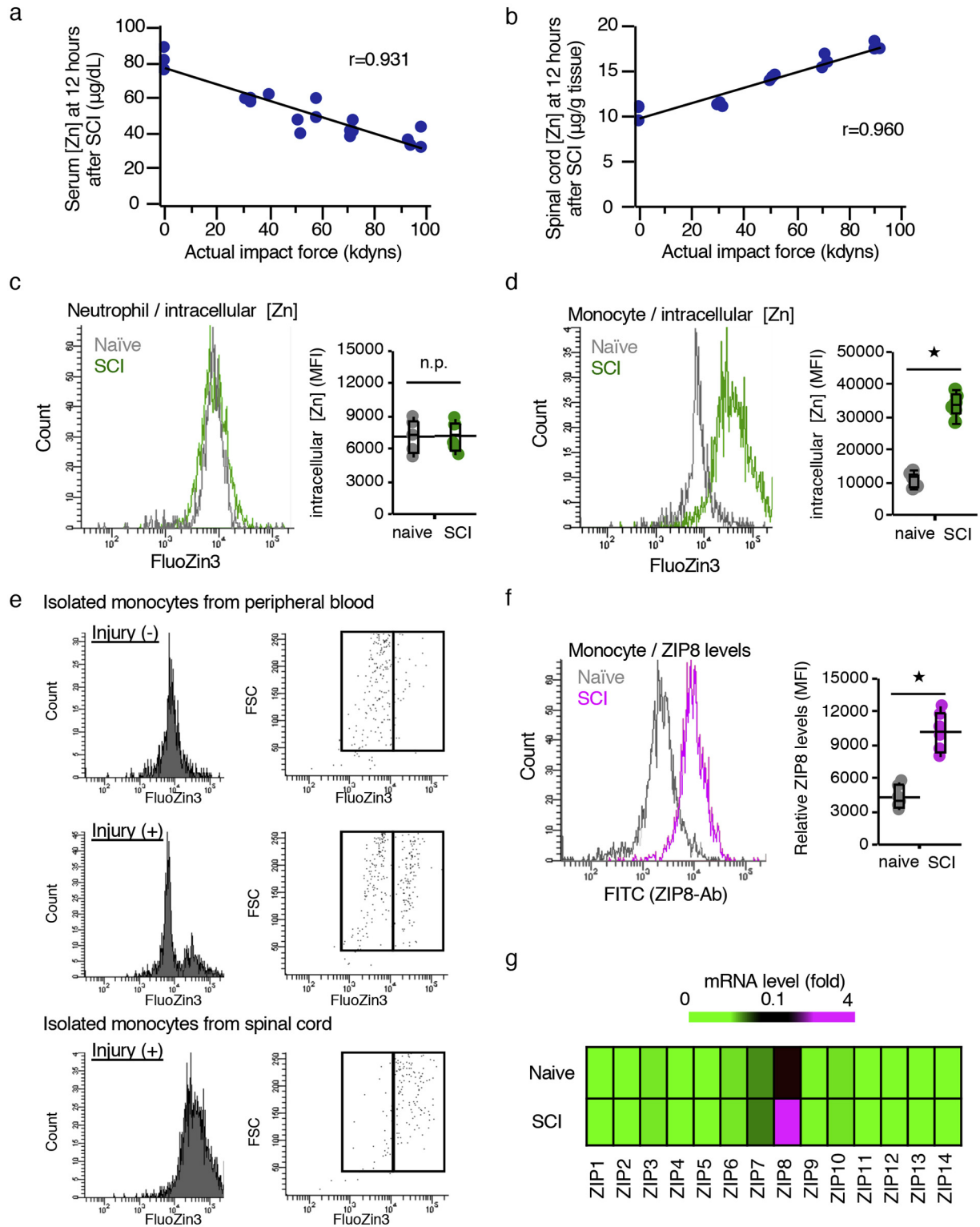
Fig. 2. Infiltrating monocytes that incorporated zinc into the cells were involved in the reduction in the serum zinc concentration. (a) The correlation between the severity of SCI and the serum zinc concentration at 12 h post-injury (hpi) ($n = 20$, $r = 0.9312$, $P < 0.0001$, Pearson's correlation coefficient). (b) The correlation between the severity of SCI and the spinal cord zinc concentration at 12 hpi ($n = 15$, $r = 0.9597$, $P < 0.0001$, Pearson's correlation coefficient). (c, d) A flowcytometric analysis. Mouse leukocytes were stained with CD45-PerCP/Cy5.5, CD11b-APC and Gr-1-PE/Cy7, along with FluoZin-3. Neutrophils were selected as CD45^{posi}/CD11b^{posi}/Gr-1^{high} cells and monocytes as CD45^{high}/CD11b^{posi}/Gr-1$^{nega-int}$ cells. The relative levels of intracellular zinc were compared based on the mean fluorescence intensity (MFI) ($n = 6$ per group). (e) A histogram analysis of FluoZin-3-positive cells within monocytes in peripheral blood of naïve mice, monocyte in peripheral blood of SCI mice, and infiltrated monocytes in spinal cord of SCI mice. The relative levels of zinc were compared based on the MFI ($n = 6$ per group). (f) A flowcytometric analysis. Mouse leukocytes were stained with CD45-PerCP/Cy5.5, CD11b-APC and Gr-1-PE/Cy7, along with ZIP8 antibody and Alexa Fluor 488-secondary conjugate. The relative levels of ZIP8 were compared based on the MFI ($n = 6$ per group). (g) The mRNA expression profile of all ZIPs revealed that SCI significantly increased the expression of ZIP8 in sorted monocytes/macrophages as determined by qRT-PCR. In contrast, the basal levels of the 13 other ZIPs were low, and SCI did not alter the expression of these ZIPs ($n = 4$ per group). In box-plots median (middle line), first and third quartile range (box) and interquartile range (IQR) of 1.5 (whiskers) are represented, and the long horizontal line outside box represents mean; *P < 0.05, Wilcoxon's rank sum test (c, d, and f); n.s., not significant.
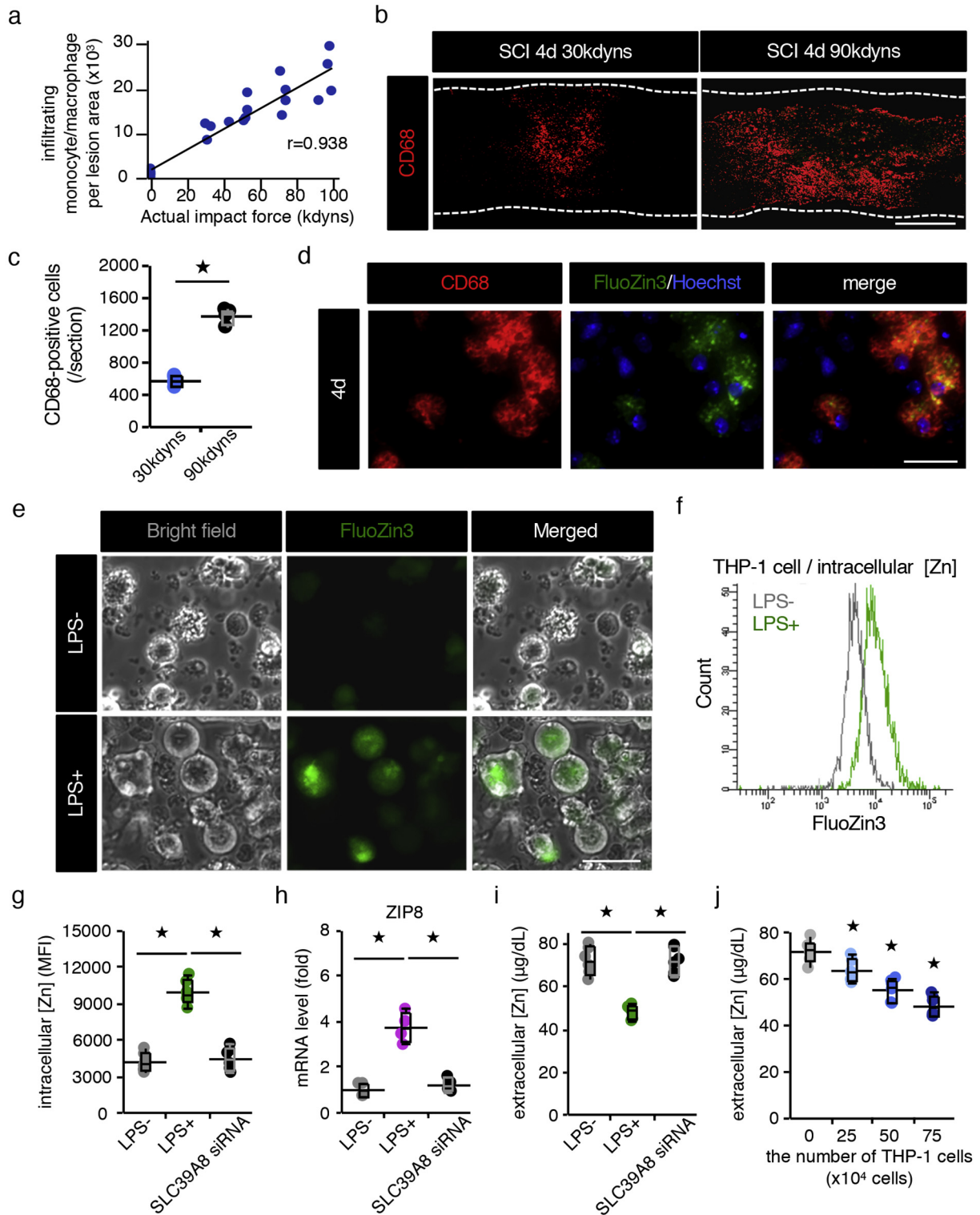
Fig. 3. The serum zinc concentration is decreased in a cell-number-dependent manner. (a) The correlation between the severity of SCI and the number of infiltrating monocytes/macrophages per lesion area at 12 hpi ($n = 22$ mice, $r = 0.9381$, $P < 0.0001$, Pearson's correlation coefficient). (b) An immunohistochemical analysis of CD68-positive infiltrated monocytes/macrophages in the lesions of 30 and 90 kdyn SCI mice at 4 dpi. (c) The quantification of FluoZin3-positive monocytes/macrophages in the 30 and 90 kdyn SCI mice at 4 dpi ($n = 4$ per group). (d) CD68 and FluoZin3 double-positive monocytes/macrophages in the lesion. The nucleus was counterstained with Hoechst 33258 dye (blue). (e) An image analysis of THP-1 cell using the cell-permeable zinc indicator FluoZin-3. Zinc influx into THP-1 cells was observed 4 h after LPS stimulation. (f) A histogram analysis of FluoZin-3-positive THP-1 cells. The intracellular zinc levels were compared based on the MFI. (g) The intracellular zinc level was quantified by flow cytometry. SLC39A8 siRNA-treated THP-1 cells were stimulated with LPS (1 mg/ml), followed by FluoZin-3 staining ($n = 6$ per group). (h) The quantification of the mRNA expression of the ZIP8 gene ($n = 4$ per group). (i) The zinc concentration in the culture medium ($n = 6$ per group). (j) The decrease in the culture medium zinc concentration in a cell-number-dependent manner ($n = 6$ per group). Scale bar = 500 μm (b), 40 μm (d), and 40 μm (e). In box-plots median (middle line), first and third quartile range (box) and interquartile range (IQR) of 1·5 (whiskers) are represented, and the long horizontal line outside box represents mean; *$P < 0.05$, Wilcoxon's rank sum test (c, g, h, and i), ANOVA with Dunnett's post hoc test (j).

expression and result in zinc influx, we evaluated the intracellular zinc concentration after LPS stimulation. Using the human monocyte cell line THP-1, our findings revealed that the intracellular zinc concentration levels and ZIP8 expression rapidly increased in response to LPS, but they were significantly impaired in ZIP8-silenced cells (Fig. 3e-h). Consistent with the increased zinc incorporation of activated monocytes, we observed a decrease in the culture medium zinc concentration, which mimics the serum zinc concentration in vivo (Fig. 3i). Furthermore, the zinc concentration in culture medium decreased in a cell-number-dependent manner after LPS stimulation (Fig. 3j), suggesting that proinflammatory stimuli cause zinc influx into monocytes and a proportional decrease in the serum zinc concentration after SCI.

3.5. Acute serum zinc concentrations predicted the functional prognosis after human SCI

Although we were able to predict the functional prognosis in the experimental mouse model, it remains unclear as to whether or not we could predict the functional prognosis in human SCI patients by evaluating the acute serum zinc concentrations. Therefore, we analyzed a human cohort of 64 SCI patients focusing on the relationship between the serum zinc concentrations at admission and the functional outcome.

After applying the inclusion/exclusion criteria, the data for 38 patients admitted within 3 days post-injury (dpi) were evaluated (Table 1). The mean period from injury to blood sampling was $1·2 \pm 0·2$ days, and the mean follow-up period was $6·3 \pm 0·8$ months. After dividing the patients into five groups based on the American Spinal Injury Association (ASIA) Impairment Scale (AIS) grade at the final follow-up, we compared the admission serum zinc concentrations of the five groups. Consequently, we revealed that the poor outcome group had significantly lower serum zinc concentrations at admission than those with better outcomes (Fig. 4a). We also examined the relationships between the admission serum zinc concentration and the ASIA motor score at final follow-up and found that there was a positive correlation between the serum zinc concentrations at admission and the ASIA motor score at final follow-up ($r = 0·858$) (Fig. 4b). Furthermore, to investigate whether or not we could predict the functional prognoses after SCI by evaluating the serum zinc concentrations at admission, we performed a non-linear regression analysis between the admission serum zinc concentrations and the final follow-up functional outcomes. The R^2 calculated by the non-linear regression equation was 0·838 (Prediction equation: AIS at final follow-up $= 98·064 / \{1 + EXP[-0·236([Zn] - 67·489)]\}$.) (Fig. 4c), which was significantly higher than any other previously reported acute biomarkers (Table 2).

Next, to investigate whether or not we could predict a patient's ability to walk independently during the acute phase of SCI, a logistic regression (LR) model based on the admission serum zinc concentrations was applied to our cohort. In this analysis, we evaluated the patients' walking abilities based on their rehabilitation records. Evaluating the admission serum zinc concentrations was extremely useful for distinguishing between those patients who were able to walk independently and those who were not (area under the curve (AUC) $= 0·974$, 95% confidence interval 0·823–0·997, $p < 0.0001$) (Fig. 4d).

Taken together, these results demonstrate that the acute serum zinc concentration is a useful biomarker for predicting the functional prognosis after human SCI.

Table 1
Clinical and epidemiological data for all patients.

| Case	Sex	Age	Mechanism of injury	Level	AIS at admission	AIS at final follow-up	Decompression surgery
1	M	52	Motor vehicle collision	C4	A	A	No
2	M	61	Motor vehicle collision	C5	D	D	Yes
3	M	68	Other accident	C5	C	D	Yes
4	F	85	Fall from height	C4	D	D	Yes
5	M	59	Fall from height	C4	C	D	No
6	F	68	Motor vehicle collision	C6	A	A	Yes
7	F	83	Fall from height	C3	A	D	No
8	F	76	Fall from height	C3	A	C	No
9	M	80	Other accident	C2	E	E	No
10	M	26	Fall from height	C7	D	D	Yes
11	M	74	Fall from height	C5	B	B	No
12	M	66	Fall from height	C5	D	D	Yes
13	F	82	Motor vehicle collision	C5	E	E	Yes
14	M	63	Fall from height	C5	C	D	No
15	M	78	Motor vehicle collision	C7	A	A	Yes
16	F	61	Motor vehicle collision	C5	C	D	Yes
17	M	68	Motor vehicle collision	C4	A	C	No
18	M	65	Fall from height	C4	E	E	Yes
19	F	22	Motor vehicle collision	C2	E	E	No
20	F	80	Other accident	C5	C	C	No
21	M	57	Other accident	C6	A	C	No
22	M	63	Fall from height	C4	C	D	No
23	M	68	Fall from height	C4	C	D	No
24	M	75	Other accident	C5	C	D	No
25	M	18	Motor vehicle collision	C4	A	B	Yes
26	M	47	Motor vehicle collision	C5	D	D	No
27	F	79	Fall from height	C5	A	C	No
28	F	83	Motor vehicle collision	C4	A	A	Yes
29	M	73	Other accident	C5	A	C	No
30	M	84	Motor vehicle collision	C5	D	D	Yes
31	M	78	Fall from height	C3	B	C	No
32	M	81	Other accident	C4	C	C	No
33	M	30	Other accident	C4	A	A	Yes
34	M	38	Other accident	C4	A	A	No
35	M	67	Fall from height	C6	C	D	No
36	M	63	Other accident	C3	D	D	No
37	M	56	Other accident	C4	D	D	No
38	M	39	Fall from height	C6	B	B	Yes
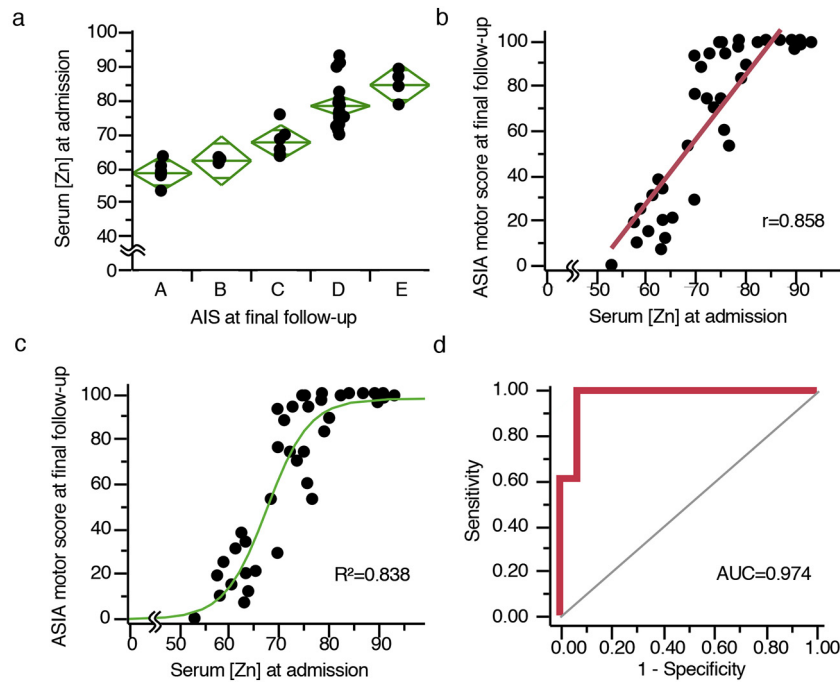
Fig. 4. The acute serum zinc concentrations predict the functional prognosis after SCI in humans. (a) The admission serum zinc concentrations of the patients with AIS at final follow-up. (b) Scatter plots illustrating the correlations between the ASIA motor score at final follow-up and the serum zinc concentration at admission ($n = 38$, $r = 0.852$, $P < 0.0001$, Pearson's correlation coefficient). (c) The results of a non-linear regression analysis of the functional outcomes using the serum zinc concentration at admission. Prediction equation: AIS at final follow-up $= 98.064 / \{1 + \text{EXP}[-0.236([Zn] - 67.489)]\}$. $R^2 = 0.838$ ($n = 38$). (d) The receiver-operating characteristics (ROC) curves of the prediction model based on admission zinc concentrations for discriminating between the ability to walk independently (with or without assisted device) or not. Area under the curve (AUC) $= 0.974$, 95% confidence interval 0.823–0.997 ($n = 38$).

4. Discussion

In this study, we reported three significant findings. First, the acute serum zinc concentration decreased in proportion to the SCI severity in a mouse experimental model. Second, we clarified the mechanism underlying this serum zinc proportional decrease in our mouse model, demonstrating that activated monocytes took up zinc from the blood serum and infiltrated the lesion in a severity-dependent manner in the acute phase of SCI. Third, in both our mouse experimental study and the human prospective cohort study, we demonstrated that the serum zinc concentration was an acute and highly-accurate biomarker for predicting the functional prognosis after SCI. These findings are useful for determining the optimum treatment strategy as well as for precisely evaluating the intervention efficacy, contributing to the development of therapies for acute SCI.

Thus far, many methods for predicting the prognosis of acute SCI have been reported; however, these previous studies have two major weak points. The first is their feasibility, as most previous prediction methods have been based on neurological examinations performed within the acute phase of SCI [35,36]. For example, van Middendorp et al. created clinical prediction rules for the ambulation prognosis by evaluating the age and some neurological findings [35]; however, immediately after injury, patients are often compromised by spinal shock, other attendant injuries, and drugs or alcohol [20,37]. Therefore, in this phase, the accurate evaluation of the neurological examination findings is extremely difficult [15,16,37,38]; in addition, their prediction model included neurological variables in the subacute phase (i.e. within the first 15 days after injury) [35]. The second weak point of these previously proposed prediction methods is their accuracy. Wilson et al. created a clinical prediction model for determining the long-term functional outcome based on acute clinical and imaging factors obtained within 3 days of injury; however, the coefficient of determination (R^2), which measures the accuracy of the model, was 0.52 [16]. Kaminski et al. created a functional outcome prediction model based on acute clinical factors, and their R^2 was 0.57 [39]. Matsushita et al. and Dalkilic et al. reported the correlation between the MRI lesion area and the neurologic prognosis, and their R^2 calculated by the correlation coefficient was 0.28 and 0.29, respectively [12,15]. In contrast, our prediction model based on the acute serum zinc concentration was able to predict the functional prognosis without any neurological examination

Table 2
A comparison of the accuracy among the acute prediction methods.

Clinical measure	Parameter	R^2	Study
ASIA motor score (6 M)	Craniocaudal diameter (mm) of intramedullary intensity changed area in MRI image at 2 or 3 days after SCI	0.28	Matsushita et al. [15]
ASIA motor score improvement (6 M)	The hematoma length and cord expansion length in MRI at 12 h after SCI	0.29	Dalkilic et al. [12]
SCIM-II score (1Y)	Age, female gender, incomplete SCI	0.31	Pouw et al. [10]
FIM motor score (1Y)	Initial AIS grade, age, and spinal MRI intramedullary signal characteristics within 3 days of injury	0.52	Wilson et al. [16]
SCIM III score (1Y)	LT, AIS grade, ISS and AMS during the acute hospitalization	0.57	Kaminski et al. [39]
ASIA motor score improvement (6 M)	Cerebrospinal fluid proteins (tau, GFAP, and S100β) at 24 h after SCI	0.58	Dalkilic et al. [12]
ASIA motor score (6 M)	Serum [Zn] within 3 days after SCI	0.84	this study

AMS = ASIA Motor Score; FIM = Functional Independence Measure; GFAP = glial fibrillary acidic protein; ISS = Injury Severity Score; LT = Light Touch score; M = Months; SCIM = Spinal Cord Independence Measure; Y = Years; [Zn] = zinc concentration.

findings. In addition, our human study exhibited a significantly high prediction accuracy in which the R^2 of the model was 0·838, even in the acute phase (at $1·2 \pm 0·2$ dpi). This accuracy was much higher than in other studies (Table 2). Therefore, the serum zinc prediction model has enough feasibility and accuracy for clinical use, overcoming the two weak points reported in previous prediction models.

The useful timing of the prognosis prediction should be the earliest possible time and when the parameters are stable. We thus examined the time course of the serum zinc concentration after SCI (70 kdyn) in the mouse experiments. As a result, we found that the serum zinc concentration exhibited the lowest value from 12 h to 3 days after injury and gradually recovered thereafter (Sup Fig. 5). Therefore, the examination timing for the serum zinc levels was decided to be at 12 h after SCI.

The ideal laboratory biomarker should be non-invasive, highly reproducible, and simple to perform [8,9]. Although measuring the serum zinc concentrations with conventional methods, such as atomic absorption spectrometry or inductively coupled plasma optical emission spectroscopy (ICP–OES), can be technically demanding, a simple and inexpensive zinc assay kit using a microplate reader has recently been developed [40]. This kit does not require a large amount of sample or any specific procedures, including acid washing treatment, thus highlighting the serum zinc concentration as a simple and easy biomarker for predicting the functional prognosis after SCI.

Regarding the mechanisms underlying the influx of Zn into monocytes, NF-κB is considered to possibly play a role. NF-κB is a transcription factor located downstream of the TLR4-mediated signaling pathway [41]. Several studies have reported that traumatic SCI brought about the activation of the TLR4/NF-κB signaling pathway in monocytes [42,43]. In addition, NF-κB has been reported to bind to the ZIP8 promoter and be associated with the Zn uptake in monocytes [32]. Given that suppression of the ZIP8 expression by siRNA significantly suppressed the zinc influx into activated monocytes in our study, we concluded that the Zn influx was up-regulated through the TLR4/NF-κB/ZIP8 pathway in infiltrating monocytes after SCI.

Under several pathological conditions, a correlation between the serum zinc concentration and disease severity has been reported. For example, Besecker et al. reported that an increase in sepsis severity was associated with a lower plasma zinc concentration [22–24]. Nangliya et al. also reported that serum zinc concentrations were correlated with the severity of liver cirrhosis [44]. In addition, Elmasry et al. reported that the serum zinc concentrations were inversely correlated with the organ failure index and organ dysfunction score in critically ill children in the pediatric intensive-care unit [45,46]. Although the mechanism of disease-related zinc concentration was unclear in these previous reports, our results suggest that amount of infiltrating monocytes with these inflammatory conditions was related with disease severity and inversely associated with the zinc serum concentration. Our results also suggest that serum zinc concentration could be feasible biomarker of pathological prognosis for another inflammatory disease conditions.

There are several potential limitations associated with our study. First, the cohort study was limited in sample size and its short follow-up period. Second, although the overwhelming majority of injured people are male, we performed all animal experiments using female mice only due to the relative ease of bladder management compared to male mice. Third, we did not examine the redistribution of zinc in other organs or cells after SCI. Zinc-redistribution has been shown in acute phase response such as trauma, infection, and cancer [47,48], which could potentially explain the alternative interpretation for low serum zinc levels in the severe SCI patients. Fourth, the BMS scale is not strictly appropriate for regression analysis, as the units represented in the scale are not approximately equal. Fifth, in the human study, we were unable to accurately determine the zinc nutritional status before the onset of SCI. Sixth, the prediction accuracy using serum zinc concentration was decreased at the subacute phase of SCI because the serum zinc concentrations gradually recovered after the subacute phase (Sup Fig. 5).

Despite these limitations, our prediction model using the serum zinc concentration showed high accuracy and feasibility in the acute phase of SCI. We believe that this biomarker will help physicians determine the optimum rehabilitation protocols within the very acute phase as well as evaluate the therapeutic intervention efficacy in clinical trials, contributing to the development of tailored therapeutic approaches for SCI.

Declaration of interests

The authors have declared that no conflict of interest exists.

Author contributions

Conception and design of the study: Y.N., S.O. Acquisition and analysis of data: S.Y., K.Y., T.S., K.K., T.M., D.K., Y.M., Drafting the manuscript and figures: M.H., K.K.

Data sharing statement

All publically available data is in this article and supplementary files.

Appendix A. Supplementary data

Supplementary data to this article can be found online at https://doi.org/10.1016/j.ebiom.2019.03.003.

References

[1] McDonald JW, Sadowsky C. Spinal-cord injury. Lancet 2002;359:417–25. https://doi.org/10.1016/S0140-6736(02)07603-1.

[2] Adams MM, Hicks AL. Spasticity after spinal cord injury. Spinal Cord 2005;43:577–86. https://doi.org/10.1038/sj.sc.3101757.

[3] Okada S, Nakamura M, Katoh H, Miyao T, Shimazaki T, Ishii K, et al. Conditional ablation of Stat3 or Socs3 discloses a dual role for reactive astrocytes after spinal cord injury. Nat Med 2006;12:829–34. https://doi.org/10.1038/nm1425.

[4] Varma AK, Das Arabinda, Wallace G, Barry John, Vertegel Alexey A, Ray Swapan K, et al. Spinal cord injury: a review of current therapy, future treatments, and basic science frontiers. Neurochem Res 2014;38:895–905. https://doi.org/10.1007/s11064-013-0991-6.Spinal.

[5] Raineteau O, Schwab ME. Plasticity of motor systems after incomplete spinal cord injury. Nat Rev Neurosci 2001;2:263–73. https://doi.org/10.1038/35067570.

[6] Rosenzweig ES, Courtine G, Jindrich DL, Brock JH, Ferguson AR, Strand SC, et al. Extensive spontaneous plasticity of corticospinal projections after primate spinal cord injury. Nat Neurosci 2010;13:1505–12. https://doi.org/10.1038/nn.2691.

[7] Rasmussen R, Carlsen EM. Spontaneous functional recovery from incomplete spinal cord injury. J Neurosci 2016;36:8535–7. https://doi.org/10.1523/JNEUROSCI.1684-16.2016.

[8] Rodrigues LF, Moura-Neto V. E Spohr TCLDS. Biomarkers in spinal cord injury: from prognosis to treatment. Mol Neurobiol 2018:1–13. https://doi.org/10.1007/s12035-017-0858-y.

[9] Pouw M, Hosman A, Van Middendorp J, Verbeek M, Vos P, Van De Meent H. Biomarkers in spinal cord injury. Spinal Cord 2009;47:519–25. https://doi.org/10.1038/sc.2008.176.

[10] Pouw MH, Hosman AJF, Van Kampen A, Hirschfeld S, Thietje R, Van De Meent H. Is the outcome in acute spinal cord ischaemia different from that in traumatic spinal cord injury? A cross-sectional analysis of the neurological and functional outcome in a cohort of 93 paraplegics. Spinal Cord 2011;49:307–12. https://doi.org/10.1038/sc.2010.114.

[11] Kuhle J, Gaiottino J, Leppert D, Petzold A, Bestwick JP, Malaspina A, et al. Serum neurofilament light chain is a biomarker of human spinal cord injury severity and outcome. J Neurol Neurosurg Psychiatry 2015;86:273–9. https://doi.org/10.1136/jnnp-2013-307454.

[12] Dalkilic T, Fallah N, Noonan VK, Salimi Elizei S, Dong K, Belanger LM, et al. Predicting injury severity and neurologic recovery after acute cervical spinal cord injury – a comparison of cerebrospinal fluid and magnetic resonance imaging biomarkers. J Neurotrauma 2017;445. https://doi.org/10.1089/neu.2017.5357 neu.2017.5357.

[13] Hayakawa K, Okazaki R, Ishii K, Ueno T, Izawa N, Tanaka Y, et al. Phosphorylated neurofilament subunit NF-H as a biomarker for evaluating the severity of spinal cord injury patients, a pilot study. Spinal Cord 2012;50:493–6. https://doi.org/10.1038/sc.2011.184.

[14] Pouw MH, Kwon BK, Verbeek MM, Vos PE, Van Kampen A, Fisher CG, et al. Structural biomarkers in the cerebrospinal fluid within 24 h after a traumatic spinal cord injury: a descriptive analysis of 16 subjects. Spinal Cord 2014;52:428–33. https://doi.org/10.1038/sc.2014.26.

[15] Matsushita A, Maeda T, Mori E, Yuge I, Kawano O, Ueta T, et al. Can the acute magnetic resonance imaging features reflect neurologic prognosis in patients with cervical spinal cord injury? Spine J 2017;17:1319–24. https://doi.org/10.1016/j.spinee.2017.05.009.

[16] Wilson JR, Grossman RG, Frankowski RF, Kiss A, Davis AM, Kulkarni AV, et al. A clinical prediction model for long-term functional outcome after traumatic spinal cord injury based on acute clinical and imaging factors. J Neurotrauma 2012;29: 2263–71. https://doi.org/10.1089/neu.2012.2417.

[17] Burns AS, Ditunno JF. Establishing prognosis and maximizing functional outcomes after spinal cord injury. Spine (Phila Pa 1976) 2001;26:S137–45. https://doi.org/10.1097/00007632-200112151-00023.

[18] Zörner B, Blanckenhorn WU, Dietz V, Curt A. Clinical algorithm for improved prediction of ambulation and patient stratification after incomplete spinal cord injury. J Neurotrauma 2010;27:241–52. https://doi.org/10.1089/neu.2009.0901.

[19] Yokota K, Saito T, Kobayakawa K, Kubota K, Hara M, Murata M, et al. The feasibility of in vivo imaging of infiltrating blood cells for predicting the functional prognosis after spinal cord injury. Sci Rep 2016;6:25673. https://doi.org/10.1038/srep25673.

[20] Hachisuka S, Kamei N, Ujigo S, Miyaki S, Yasunaga Y, Ochi M. Circulating microRNAs as biomarkers for evaluating the severity of acute spinal cord injury. Spinal Cord 2014;52:596–600. https://doi.org/10.1038/sc.2014.86.

[21] Beattie MS. Inflammation and apoptosis: linked therapeutic targets in spinal cord injury. Trends Mol Med 2004;10:580–3. https://doi.org/10.1016/j.molmed.2004.10.006.

[22] Wong HR, Shanley TP, Sakthivel B, Cvijanovich N, Lin R, Allen GL, et al. Genome-level expression profiles in pediatric septic shock indicate a role for altered zinc homeostasis in poor outcome. Physiol Genomics 2007;30:146–55. https://doi.org/10.1152/physiolgenomics.00024.2007.

[23] Cvijanovich NZ, King JC, Flori HR, Gildengorin G, Wong HR. Zinc homeostasis in pediatric critical illness. Pediatr Crit Care Med 2009;10:29–34. https://doi.org/10.1097/PCC.0b013e31819371ce.

[24] Besecker BY, Exline MC, Hollyfield J, Phillips G, DiSilvestro RA, Wewers MD, et al. A comparison of zinc metabolism, inflammation, and disease severity in critically ill infected and noninfected adults early after intensive care unit admission. Am J Clin Nutr 2011;93:1356–64. https://doi.org/10.3945/ajcn.110.008417.

[25] Moshage H. Cytokines and the hepatic acute phase response. J Pathol 1997;181: 257–66. https://doi.org/10.1002/(SICI)1096-9896(199703)181:3<257::AID-PATH756>3.0.CO;2-U.

[26] Cray C, Zaias J, Altman NH. Acute phase response in animals: a review. Comp Med 2009;59:517–26. https://doi.org/10.1002/ece3.1939.

[27] Knoell DL, Liu MJ. Impact of zinc metabolism on innate immune function in the setting of sepsis. Int J Vitam Nutr Res 2010;80:271–7. https://doi.org/10.1024/0300-9831/a000034.

[28] Scheff SW, Rabchevsky AG, Fugaccia I, Main JA, Lumpp JE. Experimental modeling of spinal cord injury: characterization of a force-defined injury device. J Neurotrauma 2003;20:179–93. https://doi.org/10.1089/08977150360547099.

[29] Ghasemlou N, Kerr BJ, David S. Tissue displacement and impact force are important contributors to outcome after spinal cord contusion injury. Exp Neurol 2005;196: 9–17. https://doi.org/10.1016/j.expneurol.2005.05.017.

[30] Basso DM, Fisher LC, Anderson AJ, Jakeman LB, Mctigue DM, Popovich PG. Basso mouse scale for locomotion detects differences in recovery after spinal cord injury

[31] Saiwai H, Ohkawa Y, Yamada H, Kumamaru H, Harada A, Okano H, et al. The LTB4-BLT1 axis mediates neutrophil infiltration and secondary injury in experimental spinal cord injury. Am J Pathol 2010;176:2352–66. https://doi.org/10.2353/ajpath.2010.090839.

[32] Liu MJ, Bao S, Gálvez-Peralta M, Pyle CJ, Rudawsky AC, Pavlovicz RE, et al. ZIP8 regulates host defense through zinc-mediated inhibition of NF-κB. Cell Rep 2013;3: 386–400. https://doi.org/10.1016/j.celrep.2013.01.009.

[33] Lucas JT, Ducker TB. Motor classification of spinal cord injuries with mobility, morbidity and recovery indices. Am Surg 1979;45:151–8.

[34] Ditunno JF, Young W, Donovan WH, Creasey G. The international standards booklet for neurological and functional classification of spinal cord injury. Am Spinal Inj Assoc Paraplegia 1994;32:70–80. https://doi.org/10.1038/sc.1994.13.

[35] van Middendorp JJ, Hosman AJF, Donders ART, Pouw MH, Ditunno JF, Curt A, et al. A clinical prediction rule for ambulation outcomes after traumatic spinal cord injury: a longitudinal cohort study. Lancet 2011;377:1004–10. https://doi.org/10.1016/S0140-6736(10)62276-3.

[36] Hicks KE, Zhao Y, Fallah N, Rivers C, Noonan V, Plashkes T, et al. A simplified clinical prediction rule for prognosticating independent walking after spinal cord injury: a prospective study from a Canadian multicenter spinal cord injury registry. Spine J 2017. https://doi.org/10.1016/j.spinee.2017.05.031.

[37] Lubieniecka JM, Streijger F, Lee JHT, Stoynov N, Liu J, Mottus R, et al. Biomarkers for severity of spinal cord injury in the cerebrospinal fluid of rats. PLoS One 2011;6: e19247. https://doi.org/10.1371/journal.pone.0019247.

[38] Brown PJ, Marino RJ, Herbison GJ, Ditunno Jr JF. The 72-hour examination as a predictor of recovery in motor complete quadriplegia. Arch Phys Med Rehabil 1991; 72:546–8.

[39] Kaminski L, Virginie C, Eduard C, Kouame M, Mac-Thiong J-M. Functional outcome prediction after traumatic spinal cord injury based on acute clinical factors. J Neurotrauma 2017;34:2027–33.

[40] Tetsuo M, Saito M, Horiguchi D, Kina K. A highly sensitive colorimetric determination of serum zinc using water-soluble pyridylazo dye. Clin Chim Acta 1982;120: 127–35. https://doi.org/10.1016/0009-8981(82)90083-3.

[41] Akira S, Takeda K. Toll-like receptor signalling. Nat Rev Immunol 2004;4:499–511. https://doi.org/10.1038/nri1391.

[42] Kigerl KA, Lai W, Rivest S, Hart RP, Satoskar AR, Popovich PG. Toll-like receptor (TLR)-2 and TLR-4 regulate inflammation, gliosis, and myelin sparing after spinal cord injury. J Neurochem 2007;102:37–50. https://doi.org/10.1111/j.1471-4159.2007.04524.x.

[43] Chen J, Wang Z, Zheng Z, Chen Y, Khor S, Shi K, et al. Neuron and microglia/macrophage-derived FGF10 activate neuronal FGFR2/PI3K/Akt signaling and inhibit microglia/macrophages TLR4/NF-κB-dependent neuroinflammation to improve functional recovery after spinal cord injury. Cell Death Dis 2017;8:e3090. https://doi.org/10.1038/cddis.2017.490.

[44] Nangliya V, Sharma A, Yadav D, Sunder S, Nijhawan S, Mishra S. Study of trace elements in liver cirrhosis patients and their role in prognosis of disease. Biol Trace Elem Res 2015;165:35–40. https://doi.org/10.1007/s12011-015-0237-3.

[45] Elmasry R, Farida Negm, Soliman D, Enas Ahmed. Assessment of serum zinc, selenium, and prolactin concentrations in critically ill children. Pediatr Heal Med Ther 2016;17. https://doi.org/10.2147/PHMT.S99191.

[46] Cirino Ruocco MA, Pacheco Cechinatti ED, Barbosa F, Navarro AM. Zinc and selenium status in critically ill patients according to severity stratification. Nutrition 2018;45: 85–9. https://doi.org/10.1016/j.nut.2017.07.009.

[47] Foster M, Samman S. Zinc and regulation of inflammatory cytokines: implications for cardiometabolic disease. Nutrients 2012;4:676–94. https://doi.org/10.3390/nu4070676.

[48] Siren PMA, Siren MJ. Systemic zinc redistribution and dyshomeostasis in cancer cachexia. J Cachexia Sarcopenia Muscle 2010;1:23–33. https://doi.org/10.1007/s13539-010-0009-z.